Revisiting Security Threat on Smart Grids: Accurate and Interpretable Fault Location Prediction and Type Classification

Carmelo Ardito[1], Yashar Deldjoo[1], Eugenio Di Sciascio[1] and Fatemeh Nazary[1]

[1]*Politecnico di Bari, Italy*

Abstract

This work revisits security threats on smart electrical grids and focuses on the dimensions of dependability, serviceability, and accountability, which constitute the security requirements of an SG application. The first two dimensions deal with fault diagnosis and location, while the last element tackles building the system more transparent. We proposed a data-driven machine-learned fault prediction system that can provide abrupt and accurate fault type classification and location prediction. Furthermore, we reported a feature interaction visualization and elaborated on how this step can facilitate interpretation of the results and assessment of the security threats in the SG. The evaluation of the system is carried out on a large-scale dataset comprised of approximately 1.9K training samples. Results show the effectiveness of the proposed system both in prediction and interpretability steps.[1]

Keywords

smart grid„ interpretability, security, fault prediction

1. Introduction and Context

Smart electrical grids – a.k.a *smart grids* (SGs) – are a complex infrastructure of distributed energy resources, appliances, and facilities that enable efficient usage, and optimization of assets, thereby reducing power consumption and investment costs. In simple terms, an SG can be viewed as an electricity market with the capacity to generate and store energy and shift load for customers [1]. Electrical grids however are susceptible to a variety of electrical abnormalities, failures, and security threats, which if not tackled abruptly, in some cases they can leave a devastating impact on lives and the country's critical industries, leading to a national dilemma. As an example, in August 2003, in the Northeast United States and Ontario, Canada, a fault occurred n the 345KV line transmission line, which triggered a cascade effect, and caused a wise-area blackout for several days. As the consequence, more than 50 million people were left without power, and an estimated loss of 4 to 10 billion dollars was induced [2, 3].

Traditionally, protection devices and circuit breakers are used to monitor faulted lines and locations [3]. However, the power outage examination report [2] outlined that undesired functioning of protective relays and circuit breakers was the main reason for the cascading

[1]Authors are listed in alphabetical order. Corresponding author: Fatemeh Nazary

ITASEC'21: Proceedings of the 15th Italian Conference on Cyber Security, April 07–09, 2021, Online event

carmelo.ardito@poliba.it (C. Ardito); yashar.deldjoo@poliba.it (Y. Deldjoo); eugenio.disciascio@poliba.it (E. D. Sciascio); fatemeh.nazary@poliba.it (F. Nazary)

effects and subsequent blackout in North America's disaster in 2003. These examples call for intelligent, fast, and accurate power system security assessment and fault diagnosis systems.

One of the key requirements of SGs is the management of electrical flow to guarantee the reliable, secure, and economical transmission of electricity. Gunduz et al. [1] outline certain security objectives that have to be satisfied to ensure security in an SG, they include confidentiality, integrity, and availability — or *the CIA triad*. Confidentiality refers to the protection of data from unauthorized disclosure. Integrity refers to the prevention of data from unauthorized alteration and destruction, and availability means accessibility of data to authorized parties in the SG when needed without compromising security. Typical cyber-attacks in SG applications target at least one of the CIA triad. In this work, we focus our attention on availability threats defined in this work as electrical faults that can occur in the distribution line, causing interruption or delay to the power delivery to consumers.

In addition to the security objectives of the CIA triad, there are certain *security requirements* that need to be fulfilled to ensure cyber-security in SG applications. They include authentication, accountability, privacy, dependability, survivability among others [1]. We focus our attention on the dimensions *dependability*, *survivability* and *accountability*, and study them in a real-life simulation of electrical grid and fault scenario. Dependability is the capacity of the system to deliver its services in-time and accurate manner, and that services be delivered even during fault periods. A requirement for ensuring dependability includes fault detection, fault forecasting, and fault prevention. Survivability aims to deliver services both in the existence of malicious activities and external faults. Fault location, maintainability, and security policies are among prominent measures for survivability. Accountability operations allow understanding who is responsible for a problem in the times they emerge, which is achieved by providing more transparent evidence about the grid functioning.

Motivated by this observation, in this work we present a data-driven self-healing system using machine learning (ML) techniques that can perform automatic and timely detection technologies of fault types and locations. Furthermore, the proposed system can keep human operators informed about why certain decisions were made by producing an interpretable visualization of the outcome. We try to answer the following research questions throughout this work.

- ***W**hat* is the fault type occurred in the electrical grid? known as the *fault type classification (FTC)* problem.
- ***W**here* the fault has occurred within the electrical grid network? known as the *fault location prediction (FLP)* problem.
- ***W**hy* the ML system made certain FLP, or FTC decisions? known as the *interpretability* problem.

FTC and FLP enable isolation of the faulty region from the rest of the grid, via providing necessary information regarding fault location and its characteristics, which expedites the required repair works (survivability and dependability). The interpretability step however aims to keep human operators involved in the control loop, by designing *interpretable* ML models that can replace the black-box prediction models and produce rules that can be understood with little inspection (accountability).

Recent literature for developing self-healing features on SGs has concentrated on machine learning (ML) and transform domain for feature extraction as an input of ML system to predict the location of the fault. In this regard, the most popular approaches for feature extraction apply transform domain such as Discrete Fourier transform (DFT) [4] whose goal is to identify fault location in presence of fault or attack. Some other works [5, 6, 7] apply Discrete wavelet transform (DWT) to address the FLP and FTC problems.

The contributions of this work are multi-fold:

1. **Information processing and prediction**: for given measurement of the three-phase voltage signals (one of the phase), extracted features from *time*, *frequency*, and *wavelet* domains. For feature representation, we investigate the impact of several statistical aggregation function including compute the n-th moment of the probability distribution functions (PDFs) [8] ($n \in [1, 4]$) together with the *energy* and *maximum* level of the signals. Further, we explore the predictive power of large class of linear and non-linear classifiers (5 classifiers in total) on the above features. Compared with the prior literature, this work investigates the impact of a large suite of factors such as the feature domain, aggregation function for feature representation and the core classifier, which makes the insights obtained very useful.
2. **Interpretability**: To better facilitate the interpretability of the black-box ML model (classifier), we utilize a model-dependent *feature importance* measurement and visualize the impact of features and their pairwise relationship on the classification outcome. In particular, the proposed interpretability apporach would allow us to answer fundamental questions about which feature class (time, frequency, or wavelet), and which statistical aggregation operator (e.g., mean, norm, skewness) are the key to building discriminative feature descriptors for the classification task.
3. **Large scale dataset:** Unlike prior works, we make use of a large scale dataset (containing 1848 measurements) to report the final results obtained.

The proposed FTC and FLP system in this work moves several steps forward our previous effort in [9] along the following directions:

- In [9], we addressed only the FTC problem. In this work, we address **both FTC and FLP tasks**.
- In [9], we used time and frequency representation analysis. Here, we use **time**, **frequency**, and **wavelet** representations.
- In [9], for the interpretability analysis, we only showed the possibility of using interaction plots. Due to space limitation, we did not provide details about what these interpretrations actually are. In this work, we provide a **deeper analysis** of the interpretability step and mention exactly **which insights** this step provides us about the impact of feature classes, and statistical aggregation operators, used for feature representation.
- Previously our dataset was comprised of 140 training instances. In this work, we use a dataset including 1848 samples, that is approximately 12 times bigger in size. This would increase the validity of the results. Furthermore, to make the work reproducible, we plan to release the dataset online.

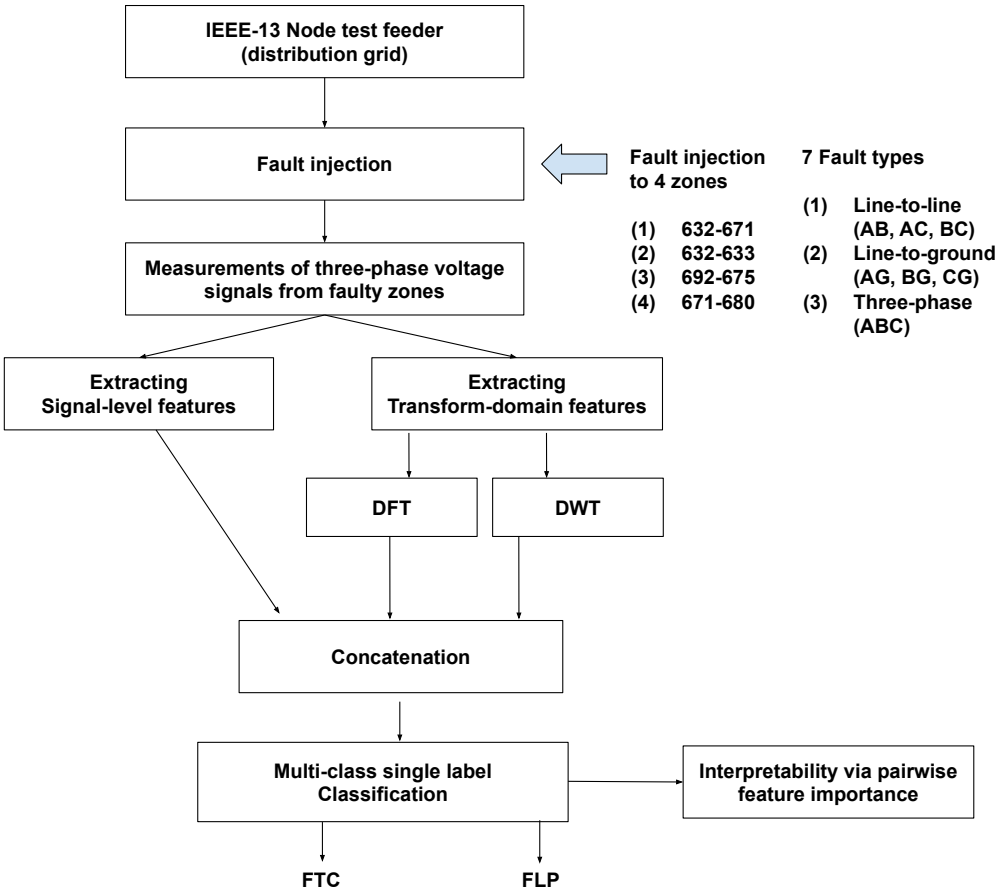

Figure 1: The flowchart of the proposed system

2. Proposed method

The proposed system in this work takes as the input a voltage signal, representing a voltage measurement of the IEEE-13 node test feeder taken from certain phase (A, B, or C) and zone in the grid, and produce as output two score related to sub-tasks: FLP (zone 1, 2, 3, and 4) and FTC, line-to-ground (AG, BG, CG), Line-to-Line (AB, AC, BC), and three-phase fault (ABC). It further produces a visualization of pairwise interaction of features on the classification outcome, providing a global understanding of the role of different feature types and representation techniques. The pipeline of processing steps (feature extraction and representation), classification, and interpretability is shown in Figure 1.

2.1. Fault simulation and Feature Extraction

For simulation, we made use of the IEEE-13 node test feeder, which is a distribution network operating at 4.16 kV. It consists of a set of characteristics that are in common with actual

networks such as unbalanced loads, voltage regulators etc [10]. We divided the network into four critical zones, i.e. (1) zone 1: 632-671; (2) zone 2: 632-633; (3) zone 3: 692-675; and (4) zone 4: 671-680. Faults were injected to all of the identified zones. Then three-phase voltage signals were measured from all that zones. To model FTC, we injected seven different short circuit faults (i.e., AG, BG, CG, AB, BC, AC, ABC) into each zone and for each fault type and zone, 22 measurements were collected corresponding to 22 resistance values fault resistance R_f values in the range [0.001-2]. The entire simulation time was set to $t = [0 - 0.022]$ seconds where faults have been injected at a certain start time $t = 0.01$ and revoked at $t = 0.02$ for all the experimental case, therefore, $t_f = [0.01 - 0.02]$ represents the *faulty period* while $t_n = [0 - 0.01]$ indicates the *normal period*. For feature extraction, for having a relative feature values, all the features extracted from the faulty period t_f were normalized by the same feature which was extracted from the non-faulty (normal) period t_n.

The key step toward successful ML-based prediction is *(i)* definition and *(ii)* extraction and representation of features that are descriminative of the respective task at hand (e.g., FTC, FLP). In this work, we chose three categories of features that were used in prior literature with different attention level [5, 6, 11, 12, 13]:

- **Time-domain:** it refers to the original data measured in time domain. For the given voltage signal $x(t)$, six aggregation functions were applied to produce a feature vector of dimensionality six to represent the time domain feature vector.
- **Discrete Fourier transform (DFT):** to obtain richer information about frequency, voltage signals were also transformed to the frequency-domain by applying discrete DFT according to $X(f) = \mathscr{F}(x(t))$, where $\mathscr{F}$ denotes the DFT operation. Afterwards, the same six aggregation functions used in the time domain were applied to the computed spectrum, to produce a feature vector of dimensionality six for the frequency-domain signal.
- **Discrete Wavelet transform (DWT)**: DWT is a digital signal processing technique that applies the concept of multi-resolution analysis to the signals [14]. In contrast to DFT, the DWT uses short window at high frequencies and long window for low frequencies, thus closely capturing characteristics of the (non-stationary) signals. In multi-resolution analysis, at decomposition level i, there are approximation A_i and detail D_i, wavelet coefficients. Motivated by prior works [6, 5], we use a high number of level-decomposition (five), and use A_5, $D_{1:5}$.

After representing each feature in the respective domain (time, frequency or wavelet), we calculate the following statistics to represent a feature in the specific domain. The statistics are obtained by applying similar aggregation functions to all signals.

- The maximum value of $x(t)$
- The energy of $x(t)$
- The first moment (mean) value of $x(t)$
- The second moment (standard deviation) value of $x(t)$
- The third moment (skewness) value of $x(t)$
- The forth moment (kurtosis) value of $x(t)$

- The maximum value of $X(f)$
- The energy of $X(f)$
- The first moment (mean) value of $X(f)$
- The second moment (standard deviation) value of $X(f)$
- The third moment (skewness) value of $X(f)$
- The forth moment (kurtosis) value of $X(f)$
- The maximum value of the coefficients: A_5 and $D_{1:5}$
- The energy of the coefficients: A_5 and $D_{1:5}$
- The first moment (mean) value of the coefficients: A_5 and $D_{1:5}$
- The second moment (standard deviation) value of coefficients: A_5 and $D_{1:5}$
- The third moment (skewness) value coefficients: A_5 and $D_{1:5}$
- The forth moment (kurtosis) value coefficients: A_5 and $D_{1:5}$

Thus, the dimensionality of the feature vectors in the time and frequency domain is 6 of the time and frequency domain. For the wavelet, we use 6 (coefficients) × 6 (aggregation operations) producing a feature vector of dimensionality 36 for the wavelet domain. These feature would constitute the main features used in the classification tasks, which we use them individually or in combination.

2.2. Fault type classification and fault location prediction

In this work, we further extend our previous work [9], in terms of the core classification task, and the classifiers' choices to perform that specific task. As for the core task, we try both fault type classification (FTC) and fault location prediction (FLP), which both are essentially multi-class classification problems. We make use of a suite of classifiers ranging from Decision-Tree, SVM, to KNN, and Ensemble methods (Bagged-Tree, subspace k-nearest neighbors).

2.3. Interpretability

Methods for ML interpretability aim to make the decision made by the ML model more transparent and provide insight into why certain decisions were made. The methods for interpretability can be generally coupled or decoupled from the decision model (i.e., the classifier). In this work, we made use of a *decision-model informed* approach for interpretability, involving visualizing the impact of pairs of features that have the highest impact on the classification task. In other words, we fixed one of the best winning classifiers in the previous task, and search for the best pairs of features that produce the highest classification accuracy. We enumerated all the possible pairs and performed the outcome classification and visualized the result using a heatmap visualization.

3. Experimental setup

In this section, we explain the experimental setup in detail such as dataset (cf. Section 3.1), the training setup and classifiers (cf. Section 3.2) that are used to validate the performance of the proposed system.

3.1. Dataset

As mentioned in Section 2.1, for data collection and creating the training dataset, the distribution system (IEEE-13) is divided into four critical zones. Afterwards, seven different faults were injected into all zones. To augment the training dataset with further data, the data collection was repeated for 22 different fault resistance values R_f in the range of 0.001 to 2 for each type of fault as listed in Table 1. Finally, three-phase voltage signals were measured independently as individual signals. As the result of these steps, in total 4 (zones) × 7 (faults) × 3 (phases) × 22 (resistance values) = 1848 training instances were created, which represent the size of the dataset used in this work for the empirical evaluation.

3.2. Classifiers and training setup

Five different classifiers were applied for FTC and FLP tasks which include: (i) Decision tree (DT), (ii) support vector machine (SVM), (iii) k-nearest neighbors, (iv) ensemble (bagged tree), and (v) ensemble (subspace KNN). For the ensemble (bagged tree) classifier, the learner type was the decision tree and the number of learners was equal to 30. Likewise, for ensemble (subspace KNN), the number of learners was set to 30 and the subspace dimension was equal to 18. To speed up the experiments, we used a hold-out validation (80%-20%) for training and test set. The exact statistics of the training and test set are shown in Table 2. We used MATLAB for feature extraction and classification experiments.

Table 1
characteristic of fault types, locations, and resistances.

Item	Details
Fault type	phase to ground AG, BG, CG
	phase to phase AB, AC, BC
	three phase ABC
Fault location	zone 1 branch 632-671
	zone 2 branch 632-633
	zone 3 branch 692-675
	zone 4 branch 671-680
Fault resistance	0.0010, 0.0273, 0.0535, 0.0798
	0.1061, 0.1323 0.1586, 0.1848
	0.2111, 0.2374, 0.2636, 0.2899
	0.3162, 0.3424, 0.3687, 0.3949
	0.4212, 0.4475, 0.4737, 0.5, 1, 2

Table 2
IEEE-13 dataset: $|\mathscr{D}|_T$ — total number of data in dataset, $|\mathscr{D}|_{Tr}$ — number of samples in training, $|\mathscr{D}|_{Te}$ — number of samples in testing.

dataset	$\lvert\mathscr{D}\rvert_T$	$\lvert\mathscr{D}\rvert_{Tr}$	$\lvert\mathscr{D}\rvert_{Te}$
IEEE-13	1848	1478	370

4. Results and discussions

We discuss the results of empirical evaluation of the proposed system through two main sub-tasks, the classification step, and the interpretability analysis, as presented in the following.

Classification: Table 3 summarizes the classification results using five classifiers for the FLP and FTC tasks based on the three feature classes, i.e., *Time*, *DFT*, *DWT* studied in this work.

On average, DWT produces the highest classification accuracy, for all the experimental cases. Time-based is ranked second and DFT produces the lowest quality. DFT produces a better result than the time-domain signal only with SVM and for the FTC task. This can be explained by the fact, DWT exploits a multi-resolution analysis, and thus it can be seen as a time-frequency approach. Finally, it could be noted the highest quality of classification is achieved when all the features are combined. Thus, on average the following relation holds about the quality of different feature descriptors: $ALL > DWT > Time > DFT$. As for the classifier type, we can note that the Ensemble methods typically provide the highest quality of classification, followed by SVM, i.e., $Ensemble > SVM >$ Others.

In summary, for FLP the best results are obtained for (ALL, Ensemble subspace k-nearest neighbors) where the accuracy is 100% followed (DWT, Ensemble) with 99.7%. For FTC, the best accuracy is obtained for (ALL, SVM) with 95.4%, and Ensemble (BT) with 93.5%.

Feature analysis and interpretability: The visualization of feature importance analysis is shown in the heatmap of Figure 2. The heatmap shows the impact of both feature classes and 48 features and their pairwise relationship on fault location prediction. We chose pairwise comparison instead of a set comparison between three or more features in order to simplify the study, because that it is easy to visualize two feature interactions on a 2D space. We show the results of FLP with *decision tree* classifier for the interpretability analysis. We answer the following experimental questions with the interpretability analysis:

Q1. Which feature classes (domains) have the most impact on the prediction task? according to Figure 2, it can be noted that most of the orange and yellow regions which correspond to highly accurate classification outcomes are related to DWT. In other words, it is interesting to understand that the DWT feature class contains more discriminative information (and in particular for $d1$ and $d2$) in comparison with the time and frequency domain which are mostly blue-colored (regardless of the feature aggregation method). These results provide more transparent information about details of the ML prediction, and that in fact, DWT contains more useful information compared with DFT and time signal, thanks to its multi-resolution analysis and the filter bank.

Q2. Which aggregation functions (norm, mean, skewness, etc.) used for the feature representation improve the classification accuracy the most? if we look at the results in DWT part we can note that interestingly majority of yellow regions belong to $Kurtois > skewness > Mean$. These results are insightful and reflect the importance of n-th moment PDF statistics.

Q3. Which is the best interaction between domains and extracted features? we can note that the general observation is that the interaction of DWT with other classes (DWT, DFT, and time) improve the classification accuracy. However, the interaction of DFT and time does not provide much useful information to classification. Finally, we can note that the best results are obtained for (DWT, skewness, d1, and d2) and (DWT, kurtosis, d1, and d2).

Table 3
Classification accuracy (%) using 48 (6+6+36) features and five classifiers. The first and second best results are shown in Bold and Italic, respectively.

Domain	Classifier	FLP	FTC
Time	DT	67.5	88.1
	SVM	59.1	90.5
	KNN	58	86.2
	Ensemble (BT)	72.1	88.3
	Ensemble (K)	63.1	88.9
Frequency (DFT)	DT	59.1	82.4
	SVM	59.3	91.6
	KNN	62.3	85.1
	Ensemble (BT)	65	87.3
	Ensemble (K)	59.9	83.2
Wavelet (DWT)	DT	99.2	92.1
	SVM	98.9	93
	KNN	98.6	93
	Ensemble (BT)	*99.7*	*93.5*
	Ensemble (K)	*99.7*	84.8
All	DT	*99.7*	94.3
	SVM	98.6	**95.4**
	KNN	97.3	92.4
	Ensemble (BT)	99.5	94.9
	Ensemble (K)	**100**	84.8

5. Conclusion and future work

In this paper, we have addressed the security threats on the electrical grid, representing one of the self-healing features for smart grids. First, we created a large-scale dataset composed of 1.8K samples by injecting faults to the IEEE-13 distribution network and collecting data; second, we built a data-driven approach to perform fault location detection (FLD) and fault type classification (FTC) automatically and accurately. Our proposed approach relies on a suite of features extracted from time, frequency, and more importantly wavelet domain. It also makes use of several state-of-the-art classification techniques to test and measure the importance of different feature classes. We further explored the role of different aggression functions for feature representation. Finally, a distinctive contribution of this paper is to provide an interpretability analysis for the above classification task in which we shed light on how interpretability can provide evidence about why certain decision makings were made by the ML system. Results are promising and witness the merits of the the proposed system to tackle security issues in SGs. In future, we plan to investigate on the efficacy of the proposed system on larger-sized IEEE node test feeders. In addition, designing similar system for detection of (deliberate) attacks such as the ones based on adversarial machine learning [15] — or adversarial attacks — constitutes another interesting open research challenge for future.

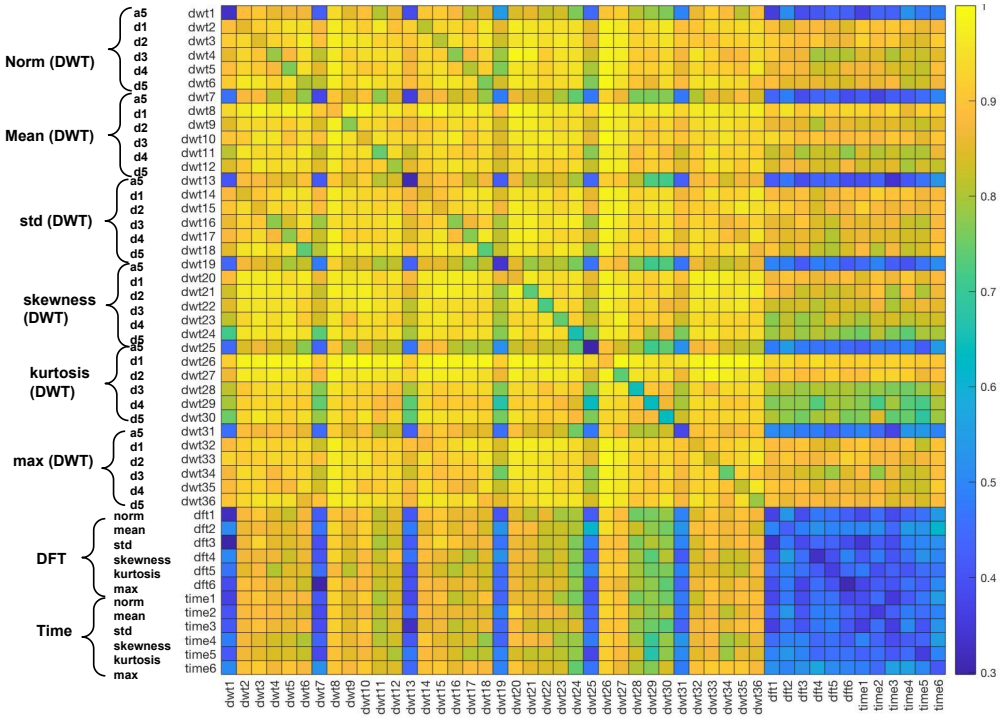

Figure 2: Visualization of the interaction of different features on the FLP classification results measured in terms of accuracy. In total, the impact of pairwise interaction of 48 features is shown in this figure.

Acknowledgments

This work has been partially funded by *e-distribuzione S.p.A* company, Italy, through a PhD scholarship granted to Fatemeh Nazary.

The authors also acknowledge partial support of the projects: Servizi Locali 2.0, PON ARS01-00876 Bio-D, PON ARS01-00821 FLET4.0, PON ARS01-00917 OK-INSAID, H2020 PASSPARTOUT.

References

[1] M. Z. Gunduz, R. Das, Cyber-security on smart grid: Threats and potential solutions, Computer networks 169 (2020) 107094.

[2] D. Burpee, H. Dabaghi, L. Jackson, F. Kwamena, J. Richter, T. Rusnov, K. Friedman, L. Mansueti, D. Meyer, Us-canada power system outage task force: final report on the implementation of task force recommendations (2006).

[3] M. Majidi, M. Etezadi-Amoli, M. S. Fadali, A sparse-data-driven approach for fault location in transmission networks, IEEE Trans. Smart Grid 8 (2017) 548–556. URL: https://doi.org/10.1109/TSG.2015.2493545. doi:10.1109/TSG.2015.2493545.

[4] S. Amini, F. Pasqualetti, M. Abbaszadeh, H. M. Rad, Hierarchical location identification of destabilizing faults and attacks in power systems: A frequency-domain approach, IEEE

Trans. Smart Grid 10 (2019) 2036–2045. URL: https://doi.org/10.1109/TSG.2017.2787690. doi:10.1109/TSG.2017.2787690.

[5] J. J. Q. Yu, Y. Hou, A. Y. S. Lam, V. O. K. Li, Intelligent fault detection scheme for microgrids with wavelet-based deep neural networks, IEEE Trans. Smart Grid 10 (2019) 1694–1703. URL: https://doi.org/10.1109/TSG.2017.2776310. doi:10.1109/TSG.2017.2776310.

[6] T. S. Abdelgayed, W. G. Morsi, T. S. Sidhu, A new harmony search approach for optimal wavelets applied to fault classification, IEEE Trans. Smart Grid 9 (2018) 521–529. URL: https://doi.org/10.1109/TSG.2016.2555141. doi:10.1109/TSG.2016.2555141.

[7] V. Veerasamy, N. I. A. Wahab, R. Ramachandran, M. Thirumeni, C. Subramanian, M. L. Othman, H. Hizam, High-impedance fault detection in medium-voltage distribution network using computational intelligence-based classifiers, Neural Computing and Applications 31 (2019) 9127–9143.

[8] A. Spanos, Probability Theory and Statistical Inference: Empirical Modeling with Observational Data, Cambridge University Press, 2019.

[9] C. Ardito, Y. Deldjoo, E. D. Sciascio, F. Nazary, Interacting with features: Visual inspection of black-box fault type classification systems in electrical grids, in: Proceedings of the Italian Workshop on Explainable Artificial Intelligence co-located with 19th International Conference of the Italian Association for Artificial Intelligence, XAI.it@AIxIA 2020, Online Event, November 25-26, 2020, 2020, pp. 135–141. URL: http://ceur-ws.org/Vol-2742/short8.pdf.

[10] F. E. Postigo Marcos, C. Mateo Domingo, T. Gomez San Roman, B. Palmintier, B.-M. Hodge, V. Krishnan, F. de Cuadra García, B. Mather, A review of power distribution test feeders in the united states and the need for synthetic representative networks, Energies 10 (2017) 1896.

[11] Q. Cui, Y. Weng, Enhance high impedance fault detection and location accuracy via -pmus, IEEE Trans. Smart Grid 11 (2020) 797–809. URL: https://doi.org/10.1109/TSG.2019.2926668. doi:10.1109/TSG.2019.2926668.

[12] E. A. Reche, J. V. de Sousa, D. V. Coury, R. A. S. Fernandes, Data mining-based method to reduce multiple estimation for fault location in radial distribution systems, IEEE Trans. Smart Grid 10 (2019) 3612–3619. URL: https://doi.org/10.1109/TSG.2018.2832840. doi:10.1109/TSG.2018.2832840.

[13] V. Veerasamy, N. I. A. Wahab, R. Ramachandran, M. Thirumeni, C. Subramanian, M. L. Othman, H. Hizam, High-impedance fault detection in medium-voltage distribution network using computational intelligence-based classifiers, Neural Comput. Appl. 31 (2019) 9127–9143. URL: https://doi.org/10.1007/s00521-019-04445-w. doi:10.1007/s00521-019-04445-w.

[14] S. Mallat, A theory for multiresolution signal decomposition: The wavelet representation, IEEE Trans. Pattern Anal. Mach. Intell. 11 (1989) 674–693. URL: https://doi.org/10.1109/34.192463. doi:10.1109/34.192463.

[15] Y. Deldjoo, T. D. Noia, F. A. Merra, A survey on adversarial recommender systems: from attack/defense strategies to generative adversarial networks, ACM Computing Surveys (CSUR) 54 (2021) 1–38.